ACS APPLIED MATERIALS & INTERFACES

Research Article

www.acsami.org

Self-Assembled Free-Standing Graphene Oxide Fibers

Zhengshan Tian,[†,‡] Chunxiang Xu,[*,†] Jitao Li,[†] Gangyi Zhu,[†] Zengliang Shi,[†] and Yi Lin[†]

[†]State Key Laboratory of Bioelectronics, Southeast University, Nanjing 210096, China

[‡]School of Chemistry and Chemical Engineering, Pingdingshan University, Pingdingshan 467000, China

ABSTRACT: It is a great challenge to directly assemble two-dimensional (2D) graphene oxide (GO) sheets into 1D fibers without any polymer or surfactant for their promising multifunctional applications. Herein, a facile self-assembly strategy is proposed to fabricate neat GO fibers from cost-efficient, aqueous GO suspension at a liquid/air interface based on the repulsive electrostatic forces, attractive van der Waals forces, and $\pi-\pi$ stacking. During the self-assembly process and ultrasonic cleaning, the morphology variated from the source graphite powder through GO sheets to GO fibers and finally to neat GO fiber films. It is interesting to note that the electrical property of the GO fiber films was improved dramatically after subsequent low-temperature thermal annealing. The morphological evolution process and formation mechanism were analyzed on the basis of optical microscopy, scanning electron microscopy, and transmission electron microscopy observation, and the electrical characteristics was also discussion.

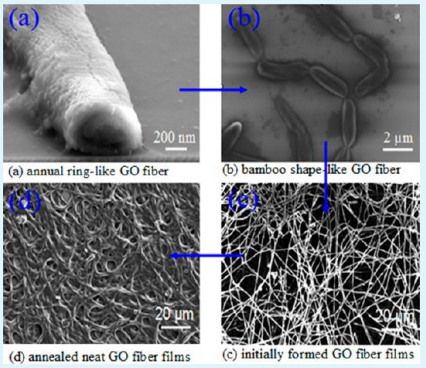

KEYWORDS: *graphene, graphene oxide, self-assembly, graphene oxide fiber, graphene oxide fiber film, thermal annealing*

1. INTRODUCTION

As a two-dimensional (2D) monolayer of carbon atoms with honeycomb lattice, graphene has been considered as a basic building block for sp^2 carbon materials of all other dimensionalities including fullerene, carbon nanotube, and graphite.[1] Since Geim et al. peeled a few graphene sheets from highly oriented pyrolytic graphite by a "scotch tape" method in 2004,[2] some fascinating properties of this conceptual matter and its derivatives, such as chiral quantum Hall effects,[3] giant intrinsic carrier mobility,[4] high thermal conductivity,[5] and extraordinary elasticity and stiffness,[6] indicate potential applications in nanocomposites with various matrixes, ultrathin membrane materials, and quantum devices. Particularly, graphene oxide (GO) sheet holds the promise for integration into various macroscopic architectures, owing to ease preparation, facile processing, scalable production, low cost, and good solubility in water and polar organic solvents.[7] Recently, graphene sheet or its derivatives have been conformably assembled into 2D macroscopic configurations such as papers,[8−10] transparent and conductive films,[11,12] and even 3D frameworks.[13,14] Moreover, the graphene-based fiber materials are of practical importance in theoretical and experimental studies, due to their promising multifunctional applications such as smart clothing, electronic wire, field emission, chemical sensors, and so on. The recently reported synthetic strategies mainly include wet-spinning the aqueous GO liquid crystals in a coagulation bath[7,15,16] or the concentrated dope of graphene and hyperbranched polyglycerol in a coagulation bath,[17] baking the aqueous GO suspension in a sealed pipeline,[18] and self-assembling the chemical vapor deposition grown graphene films[19] or the reduced GO nanoribbon.[20] However, it is a great challenge to directly assemble 2D GO sheets into 1D fibers without any polymer or surfactant, due to the lack of scalable assembly methods,[21] the size and irregular shape of chemically derived graphenes, and the movable layer-by-layer stacking of graphenes.[18] Therefore, for integration of the remarkable properties of individual graphene sheet or its derivatives into advanced, macroscopic, and functional structures for practical applications, an effective assembly strategy in a well-controlled way has to be developed.

In this paper, a facile self-assembly strategy was proposed to fabricate macroscopic neat GO fibers from cost-efficient aqueous GO suspension at the liquid/air interface. Without using any polymer or surfactant, this method is easy to scale up. The neat GO fibers show excellent flexibility, and the electrical property was improved dramatically after subsequent low-temperature thermal annealing in a sealed Teflon autoclave at 180 °C for 5 h.

2. EXPERIMENTAL SECTION

Preparation of GO Fibers. A homogeneous GO aqueous dispersion was obtained by finely controlling ultrasonication-assisted exfoliation of graphite oxide, which was synthesized from natural graphite powder by a modified Hummers' method.[22] The shapes, and dimensionalities of GO sheets and rich functional groups on their surfaces and edges are favor to functionalization. The GO fibers were formed gradually at the liquid/air interface during the two-weeks standing of the resulted stable colloid in a beaker (2000 mL) at room temperature. The initially formed GO fibers were easily transferred from the parent GO suspension onto arbitrary substrates because they were stable, free-standing and floating on the solution surface. After ultrasonic cleaning in deionized water for 1 h and subsequent drying in air at room temperature, the initially formed GO fibers turned into

Received: December 7, 2012
Accepted: January 31, 2013
Published: January 31, 2013

   dx.doi.org/10.1021/am303010j | ACS Appl. Mater. Interfaces 2013, 5, 1489−1493

neat GO fibers, and intertwined into GO fiber films before they were transferred onto a SiO_2/Si substrate. The neat GO fiber films with a SiO_2/Si substrate were thermally annealed at low temperature of 180 °C for 5 h in a sealed Teflon autoclave, and then cooled to room temperature naturally. The diameter and length of the fibers were controlled by either changing the sizes of containers or adjusting the times of ultrasonic treatment and self-assembly process. Large-scale preparation and continuous production of GO fibers were obtained by self-assembling and transferring the floating GO fibers in batches in turn.

Characterization. The morphology and structure of parent GO sheets and the fibers mentioned above were characterized by optical microscopy (OLYMPUS BX53F), scanning electron microscopy (SEM, Hitachi S-4800), Raman spectroscopy (M005−141) with an excitation laser of 514 nm, transmission electron microscopy (TEM, JEM-2100) with an acceleration voltage of 200 kV, X-ray diffractometer (XRD, Bruker D8 Discover) with Cu Ka radiation (1.5406 Å) and Fourier transform infrared spectra (FTIR, Nicolet5700). The corresponding conductivity of the annealed neat GO fiber films was measured by semiconductor parameter analyzer (KEITHLEY 4200-SCS). The Young's modulus of the GO fiber was tested by nanoindentation in an atomic force microscope (AFM, MFP-3D-SA).

3. RESULTS AND DISCUSSION

Figure 1 shows the evolvement process of the GO fiber self-assembly. It can be seen that the original aqueous GO solution

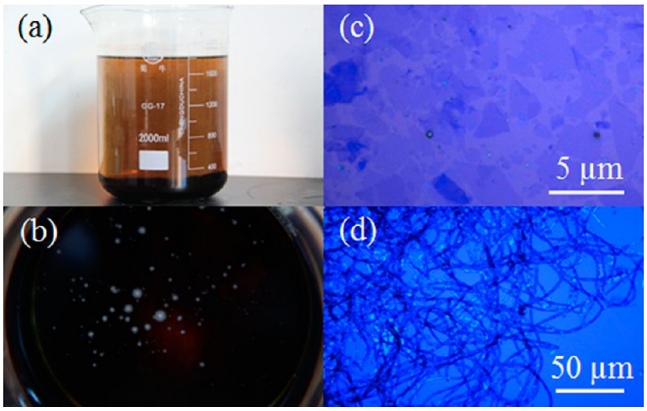

Figure 1. Evolvement process of the GO fiber self-assembly: (a) optical photograph of GO suspension, (b) optical photograph of the self-assemble product at the liquid/air interface, (c) optical microscope image of parent GO sheets, and (d) optical microscope image of neat GO fibers.

appears a light brown color, and some sedimentation emerges at the bottom of the beaker, which results from the precipitation of multilayered GO under gravity with long-time standing and supply sustaining source to maintain a fixed concentration of GO solution in the self-assembly process (Figure 1a). Remaining stationary at room temperature for two weeks, some white flecks formed gradually at the liquid/air interface, as shown in Figure 1b. The product presents intertwined fibers (Figure 1d) with a diameter of 1−2 μm and a length of about hundreds of micrometers. The diameter of the initially formed GO fibers is much smaller than that of graphene sheet fibers prepared by other routes reported at present (50−100 μm in ref 7, ~33 μm in ref 18, 20−50 μm in ref 19, and 20−40 μm in ref 20), which may be due to ultrasonication-assisted exfoliation of GO sheets in aqueous dispersion with certain small shapes and dimensionalities in the self-assembly process (Figure 1c).

The high-magnification SEM image (Figure 2a) of the parent GO sheet offers immediate evidence for peeled-off GO sheets.

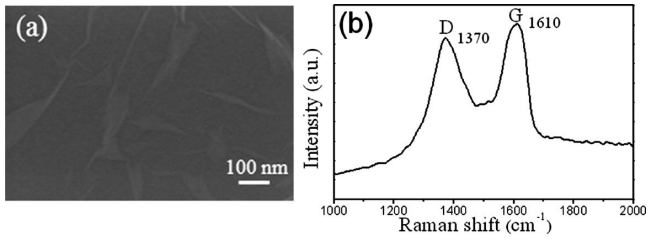

Figure 2. (a) SEM image of the parent GO sheet, and (b) Raman spectrum of the parent GO sheet.

As reported previously,[23] these as-prepared GO sheets should be mostly monolayer and few layers, individually well-dispersed in water, because of the electrostatic repulsion of the surface charge.[10] As shown in Figure 2b, the Raman spectra of GO sheet show that the G peak is at ~1610 cm^{-1} and a D peak at ~1370 cm^{-1}, indicative of the complete transformation from graphite to GO sheet.[24]

Figure 3a displays TEM image of the parent GO sheet. It can be seen that GO sheets are different levels of wrinkling and

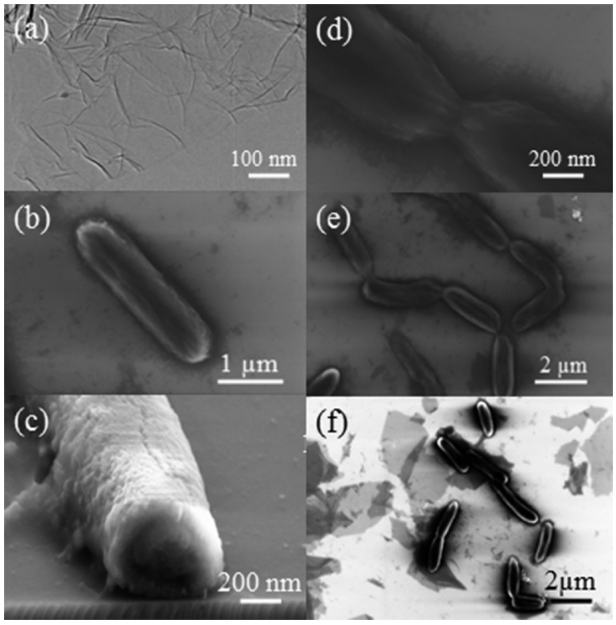

Figure 3. (a) TEM image of the parent GO sheets, (b) SEM image of a short GO fiber, (c) high-magnification SEM image of the cross-section of an individual GO fiber, (d) high-magnification SEM image of the joined part of two short GO fibers, (e) SEM image of the bamboo-like GO fiber, and (f) GO sheets under the joined short GO fibers.

'waviness', due to missing carbon atoms in the plane, and abundant functional groups, such as epoxide, hydroxyl, carbonyl, and carboxyl at the edges and in the plane, which disrupt the original conjugation and introduce lattice defects to result in folds and distortions on the sheets.[25]

It is interesting to observe that the dispersived short fibers gradually joined into a long bamboo-like structure in the surface foam, as shown the SEM images in Figure 3. The enlarged cross-section of the individual GO fiber shows an annual ring-like structure (Figure 3c). According to the observation of the

morphological evolution from GO sheet, to short fiber then to joined long fiber, a scrolling-joining-stacking manner is proposed to reveal assembly mechanism as follows. The 2D water surface is an ideal platform for self-assembling,[26] where GO sheets with certain sizes and shapes can float without surfactants or stabilizing agents. The repulsive electrostatic force[27] resists stacking of the GO sheets and results in homogeneous GO solution. At the liquid/air interface, the GO sheets scroll into short fibers with an annual ringlike structure (Figure 3b, c) due to surface tensions,[19] then join together end-to-end (Figure 3e) and grows longer and longer due to the intrinsic lamellar orientation[7] and the corresponding polarity. As new GO sheets move near to the initially formed fibers, $\pi-\pi$ stacking and van der Waals forces play a dominant role to drive them stacking each other (Figure 3f) and grow into thicker GO fibers with stable layer-by-layer structure.[27]

In situ optical microscopic images in Figure 4 also reveal the evolution process of GO fibers. Figure 4a–c are sampled in

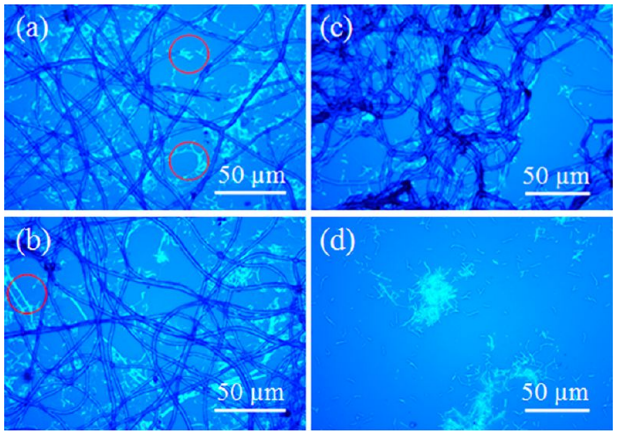

Figure 4. (a–c) In situ optical microscopic images of the assembly process obtained in turn at the 3 h interval. (d) Thinner GO fibers generated from the smaller parent GO sheets with longer ultrasonication.

turn with 3 h interval to demonstrate the diameter change of GO fiber and the amount variation of GO sheets. It is clearly seen some GO sheets and joined short fibers from the red-circles in Figure 4a. The new generated fibers circled in Figure 4b exhibited smaller diameter than that of mature fibers. The GO sheets gradually disappear from Figure 4a–c because more and more GO sheets were stacked into GO fibers as time lasting. The longer ultrasonication causes smaller parent GO sheets, and further leads to the thinner GO fibers (Figure 4d) compared to that in Figure 4c. These observations are entirely consistent with the scrolling–joining–stacking manner.

To demonstrate the effect of the ultrasonic cleaning on the morphology of the initially formed GO fibers, control experiments were carried out. We observed the surface structure and the diameter of the initially formed GO fibers before and after ultrasonic cleaning in deionized water for 1 h. It is found that the initially formed GO fibers with relative small diameter of 1.42–1.62 μm (Figure 5a) tangled together and some carbon powders interspersed among them, which were not oxidized in the modified Hummers' process. The enlarged SEM image in Figure 5c clearly illustrates some scaly GO sheets on the surface of the fiber. After ultrasonic cleaning, the neat GO fiber surface became clean, tidy, and smooth as shown in Figure 5d-f, while the diameter (1.63–1.99 μm) has a little

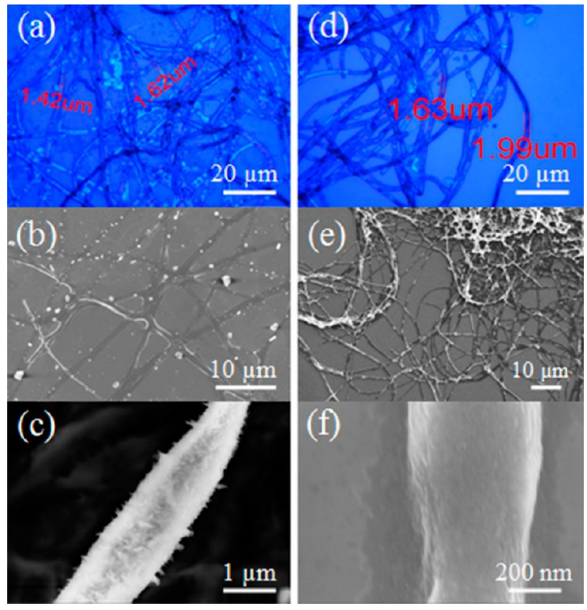

Figure 5. Morphology of the initially formed GO fibers before and after ultrasonic cleaning. (a, d) Optical microscope images of the initially formed GO fibers before and after ultrasonic cleaning; (b, e) low-magnification SEM images of the initially formed GO fibers before and after ultrasonic cleaning; (c, f) high-magnification SEM images of a single GO fiber before and after ultrasonic cleaning.

increase than that before ultrasonic cleaning because of the expansion caused by the penetration of water. Multiple twisting or folding has no damage to the obtained GO fibers, as shown in Figure 6. This indicates the mechanical stability. The Young's

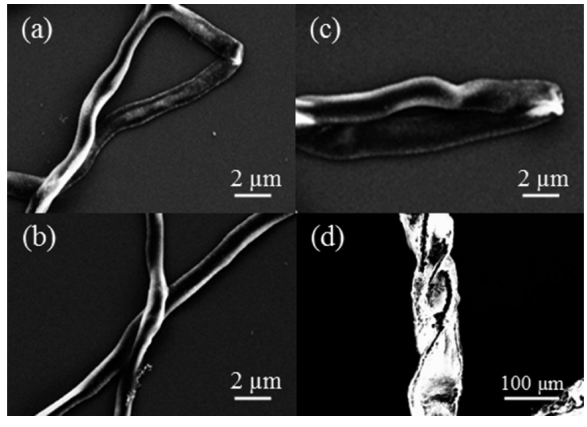

Figure 6. SEM images of (a) the twisted, (b) intercrossed, (c) folded GO fiber, and (d) a bundle of the twisted GO fibers.

modulus of the single GO fiber with a diameter of 1–2 μm is estimated as 1.1 ± 0.031 Gpa according to AFM nano-indentation measurement. This value is in the same order of magnitude with the wet-spinning assembly graphene fibers reported previously.[16] These observations demonstrate that the GO fibers maintain good structural integrity, flexibility, and resistance to torsion in the process of ultrasonic cleaning in deionized water. It is assumed that the sheet alignment, which is inherited from the intrinsic lamellar order of GO sheets, provides strong interactions between contacted sheets that are responsible for the strength of GO fibers, and the locally

dx.doi.org/10.1021/am303010j | ACS Appl. Mater. Interfaces 2013, 5, 1489–1493

crumbled structures of individual sheets make the GO fibers flexible.[7]

However, oxygen-containing functional groups attached to the GO sheet make the neat GO fibers almost electrically insulating.[28,29] Therefore, a more effective process must be developed to reduce the insulating GO fibers into highly conductive graphene fibers without destroying their original flexibility and integrity. Since the deoxygenating processes of high-temperature thermal annealing and low-temperature chemical reduction have some disadvantages,[30] we treated the neat GO fiber films at low temperature thermal annealing without any additives. Typically, after ultrasonic cleaning and subsequent drying in air at room temperature, the neat GO fiber films are annealed in a sealed autoclave at 180 °C for 5 h. As demonstrated in SEM images (Figure 7a–c), the annealed

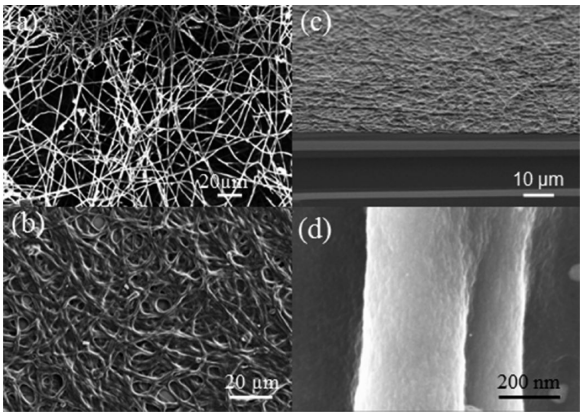

Figure 7. SEM image of (a) the as-grown and (b) annealed GO fiber films, (c) side-view of the annealed neat GO fiber films, and (d) enlarged individual annealed neat GO fiber.

neat GO fiber films are more densely intertwined compared to that without ultrasonic cleaning and annealing, and the annealed single GO fiber remains of fibrous shape with only a slight decrease in diameter (~1 μm) (Figure 7d). XRD patterns of the as-grown and annealed GO fibers are shown in Figure 8, which indicate that the interlayer spacing decreases

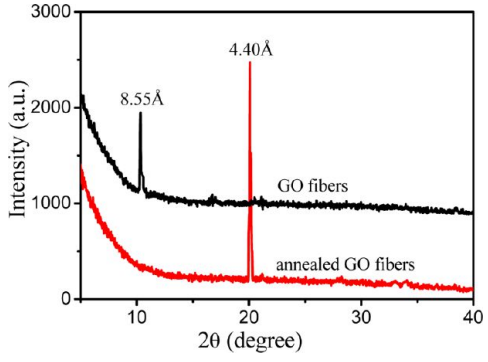

Figure 8. XRD patterns of the as-grown and annealed GO fibers.

from 8.55 Å (2θ = 10.34°) for as-grown GO fibers to 4.40 Å (2θ = 20.13°) for the annealed sample. The decrease in the interlayer spacing is attributed to the desorption of water and oxygen-containing functional groups during the thermal annealing. Similar result has also been observed in previous reports.[16,31]

To further characterize the thermal annealing and to study the nature of sp^2 domains, we performed Raman analyses on the neat GO fiber films before and after annealing, as shown in Figure 9a. One can see that only D peak (~1370 cm^{-1}) and G

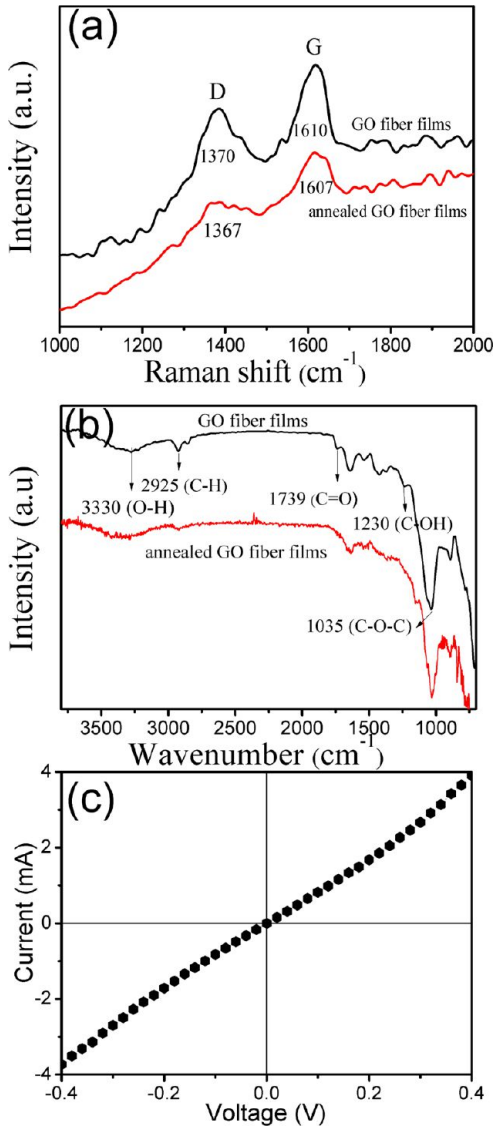

Figure 9. (a) Raman spectra of the neat GO fiber films before and after thermal annealing, (b) FTIR spectra of the neat GO fiber films before and after thermal annealing, (c) *I*–*V* curve of the annealed neat GO fiber films.

peak (~1610 cm^{-1}) are present in the neat GO fiber films. While the annealed neat GO fiber films show a relatively small enhanced G band intensity, the G peak is shifted toward lower wavenumber (~1607 cm^{-1}) compared to that of neat GO fiber films. The intensity ratio of D band (~1367 cm^{-1}) to G band (~1607 cm^{-1}) (I_D/I_G) decreases from 0.75 to 0.45 after the GO fiber film was annealed, which agrees with the previous reports,[32] suggesting a partial restoration of sp^2 carbon in the thermal annealing process.[24] The FTIR spectra have proved the presence of different oxygen-containing functional groups (Figure 9b), such as O–H stretching vibration around 3330 cm^{-1}, C–H stretching vibration around 2925 cm^{-1}, C═O stretching mode at 1739 cm^{-1}, C–OH stretching vibration at 1230 cm^{-1}, and C–O stretching mode at 1035 cm^{-1}. In

dx.doi.org/10.1021/am303010j | ACS Appl. Mater. Interfaces 2013, 5, 1489–1493

addition, the relative intensity of O−H, C−H, C═O, and C−OH decrease significantly from neat GO fiber films to annealed neat GO fiber films, implying the increase in the degree of sp^2 domains in the process of thermal annealing. The high electrical conductivity of the annealed neat GO fiber films (Figure 7c) is confirmed by two terminal current−voltage (I−V) measurements. The I−V curve of the annealed neat GO fiber films exhibits a high current flow reaching ∼4 mA at an applied bias of 0.4 V with conductivity of ∼15 S/cm^{-1} (Figure 9c), and the neat GO fiber films essentially remain an insulator under the same measurement conditions, consistent with previous reports.[33−36]

Low-temperature thermal annealing removed some of the functional groups but was unable to completely repair the holes and other irreversible defects formed within the plane of the Hummers' GO sheets. In particular, the annealed neat GO fiber films without further modification showed superior electrical properties, indicative of efficient of our method for removing oxygen-containing groups and partially restoring the extended conjugated sp^2 network.

4. CONCLUSIONS

In this work, we develop a facile, eco-friendly self-assembly strategy to fabricate neat GO fibers from cost-efficient aqueous GO suspensions at the liquid/air interface. The neat GO fibers show good flexibility and the electrical property of neat GO fiber films are improved dramatically after subsequent low temperature thermal annealing. Moreover, the neat GO fibers without any additives can provide a platform for in situ and postsynthesis incorporation of various materials with unique properties into the fiber bodies for multifunctional applications such as electromagnetic shields, antennas, and batteries. Systematic investigations are underway to further clarify the nature of the self-assembly of the GO fibers, and to find unique properties for many promising multifunctional applications in the future.

AUTHOR INFORMATION

Corresponding Author

*E-mail: xcxseu@seu.edu.cn.

Notes

The authors declare no competing financial interest.

ACKNOWLEDGMENTS

This work was supported by NSFC (61275054), "973" Program (2013CB932903 and 2011CB302004), JSIS (BE2012164), and MOE (20110092130006).

REFERENCES

(1) Geim, A. K.; Novoselov, K. S. *Nat. Mater.* **2007**, *6*, 183−191.
(2) Novoselov, K. S.; Geim, A. K.; Morozov, S. V.; Jiang, D.; Zhang, Y.; Dubonos, S. V.; Grigorieva, I. V.; Firsov, A. A. *Science* **2004**, *306*, 666−669.
(3) Zhang, Y.; Tan, Y. W.; Stormer, H. L.; Kim, P. *Nature* **2005**, *438*, 201−204.
(4) Novoselov, K. S.; Geim, A. K.; Morozov, S. V.; Jiang, D.; Katsnelson, M. I.; Grigorieva, I. V.; Dubonos, S. V.; Firsov, A. A. *Nature* **2005**, *438*, 197−200.
(5) Balandin, A. A.; Ghosh, S.; Bao, W.; Calizo, I.; Teweldebrhan, D.; Miao, F.; Lau, C. N. *Nano Lett.* **2008**, *8*, 902−907.
(6) Lee, C.; Wei, X.; Kysar, J. W.; Hone, J. *Science* **2008**, *321*, 385−388.
(7) Xu, Z.; Gao, C. *Nat. Commun.* **2011**, DOI: 10.1038/ncomms1583.
(8) Dikin, D. A.; Stankovich, S.; Zimney, E. J.; Piner, R. D.; Dommett, G. H. B.; Evmenenko, G.; Nguyen, S. T.; Ruoff, R. S. *Nature* **2007**, *448*, 457−460.
(9) Chen, H.; Müller, M. B.; Gilmore, K. J.; Wallace, G. G.; Li, D. *Adv. Mater.* **2008**, *20*, 3557−3561.
(10) Li, D.; Müller, M. B.; Gilje, S.; Kaner, R. B.; Wallace, G. G. *Nat. Nanotechnol.* **2008**, *3*, 101−105.
(11) Eda, G.; Fanchini, G.; Chhowalla, M. *Nat. Nanotechnol.* **2008**, *3*, 270−274.
(12) Li, X.; Zhang, G.; Bai, X.; Sun, X.; Wang, X.; Wang, E.; Dai, H. *Nat. Nanotechnol.* **2008**, *3*, 538−542.
(13) Xu, Y.; Sheng, K.; Li, C.; Shi, G. *ACS Nano* **2010**, *4*, 4324−4330.
(14) Lee, S. H.; Kim, H. W.; Hwang, J. O.; Lee, W. J.; Kwon, J.; Bielawski, C. W.; Ruoff, R. S.; Kim, S. O. *Angew. Chem., Int. Ed.* **2010**, *122*, 10282−10286.
(15) Xu, Z.; Sun, H.; Zhao, X.; Gao, C. *Adv. Mater.* **2013**, *25*, 188−193.
(16) Cong, H. P.; Ren, X. C.; Wang, P.; Yu, S. H. *Sci. Rep.* **2012**, *2*, 613.
(17) Hu, X.; Xu, Z.; Gao, C. *Sci. Rep.* **2012**, *2*, 767.
(18) Dong, Z.; Jiang, C.; Cheng, H.; Zhao, Y.; Shi, G.; Jiang, L.; Qu, L. *Adv. Mater.* **2012**, *24*, 1856−1861.
(19) Li, X.; Zhao, T.; Wang, K.; Yang, Y.; Wei, J.; Kang, F.; Wu, D.; Zhu, H. *Langmuir* **2011**, *27*, 12164−12171.
(20) Jang, E. Y.; Carretero-Gonźalez, J.; Choi, A.; Kim, W. J.; Kozlov, M. E.; Kim, T.; Kang, T. J.; Baek, S. J.; Kim, D. W.; Park, Y. W.; Baughman, R. H.; Kim, Y. H. *Nanotechnology* **2012**, *23*, 235601−235608.
(21) Park, S.; Ruoff, R. S. *Nat. Nanotechnol.* **2009**, *4*, 217−224.
(22) Hummers, W. S.; Offeman, R. E. J. *Am. Chem. Soc.* **1958**, *80*, 1339.
(23) Ni, Z. H.; Wang, H. M.; Kasim, J.; Fan, H. M.; Yu, T.; Wu, Y. H.; Feng, Y. P.; Shen, Z. X. *Nano Lett.* **2007**, *7*, 2758−2763.
(24) Luo, D.; Zhang, G.; Liu, J.; Sun, X. *J. Phys. Chem. C* **2011**, *115*, 11327−11335.
(25) Schniepp, H. C.; Li, J. L.; McAllister, M. J.; Sai, H.; Herrera-Alonso, M.; Adamson, D. H.; Prud'homme, R. K.; Car, R.; Saville, D. A.; Aksay, I. A. *J. Phys. Chem. B* **2006**, *110*, 8535−8539.
(26) Chen, C.; Yang, Q.; Yang, Y.; Lv, W.; Wen, Y.; Hou, P. X.; Wang, M.; Cheng, H. M. *Adv. Mater.* **2009**, *21*, 3007−3011.
(27) Cote, L. J.; Kim, F.; Huang, J. J. *Am. Chem. Soc.* **2009**, *131*, 1043−1049.
(28) Boukhvalov, D. W.; Katsnelson, M. I. *J. Am. Chem. Soc.* **2008**, *130*, 10697−10701.
(29) Mkhoyan, K. A.; Contryman, A. W.; Silcox, J.; Stewart, D. A.; Eda, G.; Mattevi, C.; Miller, S.; Chhowalla, M. *Nano Lett.* **2009**, *9*, 1058−1063.
(30) Pei, S.; Zhao, J.; Du, J.; Ren, W.; Cheng, H. M. *Carbon* **2010**, *48*, 4466−4474.
(31) Park, S.; An, J.; Jung, I.; Piner, R. D.; An, S. J.; Li, X.; Velamakanni, A.; Ruoff, R. S. *Nano Lett.* **2009**, *9*, 1593−1597.
(32) Krishnamoorthy, K.; Veerapandian, M.; Mohan, R.; Kim, S. *J. Appl. Phys. A* **2012**, *106*, 501−506.
(33) Kosynkin, D. V.; Higginbotham, A. L.; Sinitskii, A.; Lomeda, J. R.; Dimiev, A.; Price, B. K.; Tour, J. M. *Nature* **2009**, *458*, 872−876.
(34) Gao, X.; Jang, J.; Nagase, S. *J. Phys. Chem. C* **2010**, *114*, 832−842.
(35) Wang, Z.; Wang, J.; Li, Z.; Gong, P.; Liu, X.; Zhang, L.; Ren, J.; Wang, H.; Yang, S. *Carbon* **2012**, *50*, 5403−5410.
(36) Zhang, L.; Chen, G.; Hedhili, M. N.; Zhang, H.; Wang, P. *Nanoscale* **2012**, *4*, 7038−7045.